



The *Arabidopsis thaliana* flower organ specification gene regulatory network determines a robust differentiation process

Yara-Elena Sánchez-Corrales^{a,1}, Elena R. Álvarez-Buylla^{a,b}, Luis Mendoza^{b,c,*}

^a Instituto de Ecología, Universidad Nacional Autónoma de México, Ciudad Universitaria, D.F. CP04510, México

^b Centro de Ciencias de la Complejidad, Universidad Nacional Autónoma de México, Ciudad Universitaria, D.F. CP04510, México

^c Instituto de Investigaciones Biomédicas, Universidad Nacional Autónoma de México, Ciudad Universitaria, D.F. CP04510, México

ARTICLE INFO

Article history:

Received 5 November 2009

Received in revised form

18 February 2010

Accepted 2 March 2010

Available online 18 March 2010

Keywords:

FOS-GRN

Flower development

Gene regulatory networks

Arabidopsis thaliana

Dynamical models

ABSTRACT

The *Arabidopsis thaliana* flower organ specification gene regulatory network (FOS-GRN) has been modeled previously as a discrete dynamical system, recovering as steady states configurations that match the genetic profiles described in primordial cells of inflorescence, sepals, petals, stamens and carpels during early flower development. In this study, we first update the FOS-GRN by adding interactions and modifying some rules according to new experimental data. A discrete model of this updated version of the network has a dynamical behavior identical to previous versions, under both wild type and mutant conditions, thus confirming its robustness. Then, we develop a continuous version of the FOS-GRN using a new methodology that builds upon previous proposals. The fixed point attractors of the discrete system are all observed in the continuous model, but the latter also contains new steady states that might correspond to genetic activation states present briefly during the early phases of flower development. We show that both the discrete and the continuous models recover the observed stable gene configurations observed in the inflorescence meristem, as well as the primordial cells of sepals, petals, stamens and carpels. Additionally, both models are subjected to perturbations in order to establish the nature of additional signals that may suffice to determine the experimentally observed order of appearance of floral organs. Our results thus describe a possible mechanism by which the network canalizes molecular signals and/or noise, thus conferring robustness to the differentiation process.

© 2010 Elsevier Ltd. All rights reserved.

1. Introduction

Dynamical gene regulatory network models have become instrumental for understanding the concerted action of groups of genes and proteins during cell differentiation and morphogenesis of diverse biological systems (see for example Álvarez-Buylla et al., 2007; Benítez et al., 2008; Huang and Ingber, 2006; Li et al., 2006; von Dassow et al., 2000). Such approach has been extensively used to understand cell differentiation during early stages of *Arabidopsis thaliana* flower development. Indeed, a flower organ specification gene regulatory network (FOS-GRN) model, which incorporates the key molecular components during cell type determination in the inflorescence and flower meristems, has been proposed (Chaos et al., 2006; Espinosa-Soto et al., 2004; Mendoza and Álvarez-Buylla, 1998; Mendoza et al., 1999).

The FOS-GRN model recovers as steady states the multigenic expression profiles or gene expression configurations that are observed in cells of the inflorescence meristems, as well as of sepals, petals, stamens and carpels primordia. Such model has been validated by simulating the floral mutants that have been described experimentally, and the model has also lead to predictions that have been later corroborated experimentally. For example, the prediction that the gene AGAMOUS should up-regulate itself (Espinosa-Soto et al., 2004), was afterwards experimentally confirmed by an independent group (Gómez-Mena et al., 2005).

In this study we first update the FOS-GRN taking into account recent published experimental data that resulted in modifications of both the topology and the logical functions of the network components. We show that the updated model still describes the observed patterns of expression in the inflorescence and flower meristems of *A. thaliana*. And second, we present a continuous version of the FOS-GRN model. Most previous versions of the model were implemented as discrete dynamical systems, in which the transcriptional activation state of a given gene was described by a binary or ternary variable as a function of the states of its regulatory inputs (Álvarez-Buylla et al., 2008;

* Corresponding author at: Instituto de Investigaciones Biomédicas, Universidad Nacional Autónoma de México, Ciudad Universitaria, D.F. CP04510, México. Tel.: +52 55 56229210.

E-mail address: lmendoza@biomedicas.unam.mx (L. Mendoza).

¹ Present address: Department of Cell and Developmental Biology, John Innes Centre, Norwich NR4 7UH, UK.

Chaos et al., 2006; Espinosa-Soto et al., 2004). More recently, the same network was developed as a continuous dynamical system (Álvarez-Buylla et al., 2008) using the Glass model of differential equations (Glass, 1975). In general, however, continuous models of the FOS-GRN have been hindered because of the scarcity of quantitative experimental data on stage-specific changes in gene expression during early flower development, thus making parameter fitting to experimental data impossible. In this case, we propose an alternative continuous model with the use of a qualitative approach that does not require parameter fitting (Mendoza and Xenarios, 2006) and that it is easier to implement and interpret than the previous approach. The continuous FOS-GRN model presented here recovers the same ten fixed point attractors as the discrete versions of the model, corresponding to the wild-type gene expression patterns of inflorescence, sepal, petal, stamen and carpel primordial cells during early flower development. This model also recovers the observed steady state configurations observed in documented gain and loss of function mutants. Finally, while the previous continuous version of the FOS-GRN was used to explore the temporal appearance of the floral attractors when subjected to noise, the present study explores the specific trajectories and sequence of signals necessary for the model to visit the attractors in the order observed in the wild type flowers.

The perturbation analysis of our FOS-GRN model shows that the network is able to direct the transition from an inflorescence to a floral primordia, following the known sequence of appearance of sepals, petals, stamens and carpels primordia. These transitions are due to the existence of multiple alternative pathways by which extracellular signals are canalized towards a relatively small number of possible responses of the network, conferring robustness to the differentiation process of flowering in *A. thaliana*.

2. Results

2.1. Dynamical behavior of the FOS-GRN discrete model

Fig. 1 shows the updated topology of the *A. thaliana* flower organ specification gene regulatory network, which incorporates the latest published experimental information regarding the regulatory interactions among the modeled genes (see Section 4). The topology of the network contains three new interactions (repressions) with respect to its previous version.

The review of recent experimental evidence regarding the regulatory interactions among the genes in the FOS-GRN resulted in the update of the Boolean functions describing the response of the nodes. Table 1 presents the latest logical rules, which

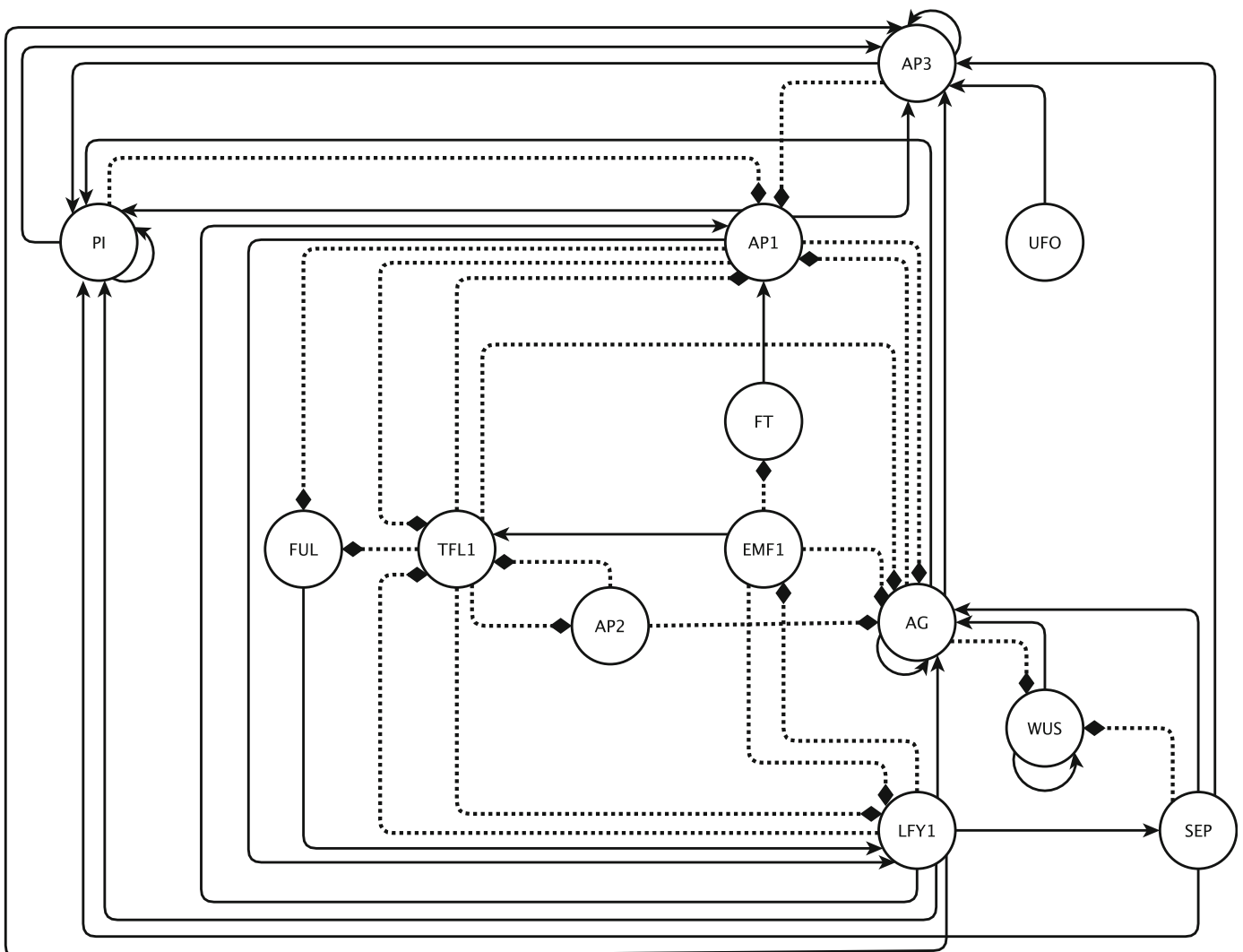


Fig. 1. The updated floral organ specification gene regulatory network (FOS-GRN) that controls the early differentiation of inflorescence and floral organs in *Arabidopsis thaliana*. Positive and negative regulatory interactions are represented by continuous and discontinuous arrows, respectively.

incorporates three new rules, corresponding to the three new interactions mentioned above. The table also contains modifications to two rules, specifically the rules for *AG* and *AP1* (see Section 4 for details).

We studied the dynamical behavior of the new version of the discrete model so as to obtain all its attractors. The network reaches ten fixed point attractors, shown in Table 2, all of which can be interpreted as a particular biological pattern of expression. It is important to note that despite the updating in the FOS-GRN, its steady states are identical to the previous discrete versions of the model (Chaos et al., 2006). Four attractors correspond to expression patterns observed in primordial cell types of inflorescence meristems, one observed in sepal primordial cells, two in petal primordial cells, two in stamen primordial cells and one in carpel primordial cells.

The basins of the ten attractors do not partition the state space equally (Table 3, central column). The four largest basins drain

Table 1
The updated logical rules of the FOS-GRN.^a

$AG = (\text{not } EMF1 \text{ and not } AP2 \text{ and not } TFL1)$ or (not EMF1 and not AP1 and LFY) or (not EMF1 and not AP2 and LFY) or (not EMF1 and not TFL1 and LFY and (AG and SEP)) or (not EMF1 and (LFY and WUS))
$AP1 = (\text{not } AG \text{ and not } TFL1)$ or (FT and LFY and not AG) or (FT and not AG and not PI) or (LFY and not AG and not PI) or (FT and not AG and not AP3) or (LFY and not AG and not AP3)
$AP2 = TFL1$ $AP3 = (LFY \text{ and } UFO)$ or ((PI and SEP and AP3 and (AG or AP1))
$EMF1 = LFY$ $FT = \text{not } EMF1$ $FUL = AP1 \text{ and not } TFL1$ $LFY = (EMF1)$ or (not TFL1)
$PI = (LFY \text{ and } (AG \text{ or } AP3))$ or ((PI and SEP and AP3 and (AG or AP1))
$SEP =$ $TFL1 = AP1 \text{ and } (EMF1 \text{ and not } LFY)$ $WUS = WUS \text{ and } (\text{not } AG \text{ or not } SEP)$

^a The state of a gene at time $t+1$ is expressed with a Boolean formula as a function of the states of its regulatory genes at time t .

Table 2
The fixed point attractors of the discrete FOS-GRN model.^a

	INF1	INF2	INF3	INF4	SEP	PET1	PET2	STM1	STM2	CAR
AG	0	0	0	0	0	0	0	1	1	1
AP1	0	0	0	0	1	1	1	0	0	0
AP2	0	0	0	0	1	1	1	1	1	1
AP3	0	0	0	0	0	1	1	1	1	0
EMF1	1	1	1	1	0	0	0	0	0	0
FT	0	0	0	0	1	1	1	1	1	1
FUL	0	0	0	0	0	0	0	1	1	1
LFY	0	0	0	0	1	1	1	1	1	1
PI	0	0	0	0	0	1	1	1	1	1
SEP	0	0	0	0	1	1	1	1	1	1
TFL1	1	1	1	1	0	0	0	0	0	0
UFO	0	1	0	1	0	1	0	1	0	0
WUS	0	0	1	1	0	0	0	0	0	0

^a The first row shows the names given to the attractors, which correspond to the expression patterns observed in different regions of the developing flower. INF1=inflorescence attractor 1, INF2=inflorescence attractor 2, INF3=inflorescence attractor 3, INF4=inflorescence attractor 4, SEP=sepal attractor, PET1=petal attractor 1, PET2=petal attractor 2, STM1=stamen attractor 1, STM2=stamen attractor 2, CAR=carpel attractor.

Table 3
Relative size of the basins of attraction with respect to the whole state space.^a

Attractor	Discrete model (%)	Continuous model (%)
INF1	1.66	4.74
INF2	1.66	4.77
INF3	0.88	4.01
INF4	0.88	4.06
SEP	9.91	11.01
PET1	10.05	12.74
PET2	0.14	1.89
STM1	37.4	28.46
STM2	1.15	6.54
CAR	36.25	21.79

^a The state space of the discrete model was explored in its entirety. In the continuous model the state space was explored by random sampling, see Section 4.

93.6% of the state space. These basins correspond to the four types of floral organs, namely: sepals, petals, stamens and carpels. In particular, the size of the basins leading to the reproductive organs, stamens and carpels, constitutes 73.6% of the state space. This feature was previously interpreted in terms of evolutionary hypotheses (Espinosa-Soto et al., 2004). One possibility is that the proportion of states leading to the reproductive organs might have been fixed by natural selection. A second possibility is that the uneven partitioning of the state space is due to historical reasons, because the sexual organs of flowers have a more ancient evolutionary origin than the perianth sterile structures.

During flower development, there is a particular order in which organs appear. Flower meristems arise in the axils of vestigial bracts that emerge at the flanks of the inflorescence meristems (see a review in Álvarez-Buylla et al., in press). Sepal primordia are determined first, as the A genes (AP1 and AP2) are turned on; then the B genes (AP3 and PI) become active, determining the petal primordial cells, and finally, the C gene (AG) is turned on determining the appearance of stamens and carpels (Smyth et al., 1990). We explored the dynamics of the discrete version of the model in order to address if it could also recover such temporal sequence of attractor emergence. Fig. 2 shows the perturbations in the nodes that result in the appearance of the attractors in the temporal sequences observed experimentally.

During the transition from inflorescence to floral primordia, *EMF1* (Chen et al., 1997; Moon et al., 2003) and *TFL1* (Shannon and Meeks-Wagner, 1993) are down-regulated, while other genes, such as *LFY* and *AP1*, are up-regulated (Shannon and Meeks-Wagner, 1993). Our model shows that it is enough to give a signal to turn *EMF1* off (Fig. 2) in order to create a cascade of signals that turn *TFL1* off, and *LFY* and *AP1* on. Thus, in our model, any internal or external signal capable of turning *EMF1* off, is able to move the whole network from the inflorescence attractor to the sepal one.

Then the transition of sepal to petal attractors depends on inducing the expression of *UFO*. This is consistent with the fact that *UFO* is expressed in the second, third and fourth whorl during flower developmental stages 2 and 3 (Laufs et al., 2003), coinciding with the appearance of petal primordia. Also, it has been shown that there is a physical interaction between the products of *UFO* and *LFY* to achieve the activation of the *AP3* gene, needed for petal development (Chae et al., 2008). An ulterior inactivation of *UFO* would still leave the system in one of the petal attractors. This explains that two attractors corresponding to the configuration of petal primordial cells were recovered.

The transition from petals to stamens can be obtained by activating *AG*, or inactivating *AP2*. Alternatively, it can be achieved by inactivating *AP1* or activating *WUS*, starting from the PET1 or PET2 attractors, respectively. Experimentally, it is known that *AG* expression is necessary for stamen development, and it is known

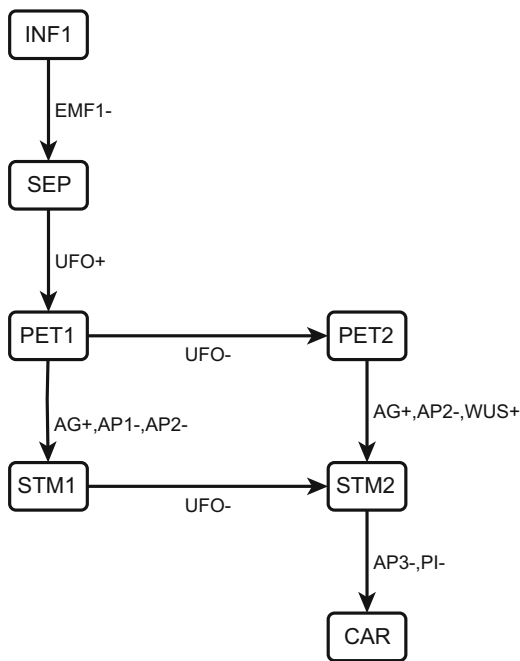


Fig. 2. Biologically relevant developmental routes of the discrete model. Each node represents a fixed point attractor (names as in Table 1), and the edge labels correspond to all the possible single-node perturbations able to move the system from one attractor to another. For example, EMF1 – means that by temporarily turning *EMF1* off in the INF1 attractor, the network moves through a series of transitory states that eventually lead the system to the SEP attractor.

that it has antagonistic activities with *AP1* and *AP2* during flower development (Deyholos and Sieburth, 2000; Drews et al., 1991; Gustafson-Brown et al., 1994; Liu and Meyerowitz, 1995). For its part, *WUS* is known to participate during flower meristem determination (Lenhard et al., 2001), but there is not enough information regarding its temporal and spatial expression to assess its relevance during the development of stamens. Notice that the difference between the two stamen attractors is only the state of activation of *UFO* (see Table 1), this is consistent with the evidence that stamens have regions either with or without expression of *UFO* (Samach et al., 1999).

Finally, regarding the change from stamen to carpel attractor, our model shows that it is necessary only to turn off either *AP3* or *PI* (see Fig. 2). This result is in agreement with the experimental evidence, because from the ABC model we know that only *AG*, and not *AP3* or *PI*, is necessary for carpel determination (Coen and Meyerowitz, 1991).

The previous paragraphs described those gene activations that are necessary for the transition from inflorescence cells to all of the floral organ primordial cells in the correct order. Nevertheless, for completeness we tested all possible single perturbations in all the attractors, shown in Fig. 3, so as to obtain a complete fate map. It is interesting to note that three out of four inflorescence attractors (INF1, INF2 and INF3) have more paths leaving from them than leading towards them. The contrary occurs for the floral attractors, where four (SEP, PET1, PET2 and CAR) out of six have more pathways leading towards them than leaving from them. This result provides a possible explanation for the fact that once flower development starts, it proceeds to completion. This characteristic constitutes an alternative way to look at robustness of the differentiation process. Specifically, attractors with small basins allow for many perturbations that may lead the system into a different attractor, while attractors with large basins catch many trajectories originated from perturbations in other attractors.

2.2. Dynamical behavior of the FOS-GRN continuous model

We implemented the FOS-GRN as a continuous dynamical system, using a modification of the standardized qualitative dynamical systems methodology (see Section 4 for details). This approach describes the state of a node with one continuous variable, in contrast to a previous model (Álvarez-Buylla et al., 2008), where there are two variables associated with every node, one to describe the level of expression, another to describe the state of expression of a gene. Running the equations from 50,000 random initial states, the system reached 10 fixed point attractors, shown in Table 4. Importantly, the attractors are the same as in the discrete version of the model (see Table 1). Furthermore, the relative sizes of the basins are also very similar between the discrete and continuous models (see Table 3). These results show that the dynamical behavior of the FOS-GRN is largely determined by the topology of the network, rather than by the detail of the kinetic functions, as had been suggested by previous analyses (Espinosa-Soto et al., 2004).

An important characteristic of continuous dynamical systems is that, contrary to discrete systems, there is an infinite number of possible initial states. Therefore, the search for attractors by sampling a large number of initial states is necessarily incomplete, and there is always the possibility of missing attractors with small basins of attraction. To find possible missing attractors we made an exhaustive perturbation study, temporarily modifying the value of each node, one by one, in all attractors (see Section 4). The result is the fate map shown in Fig. 4, which is the continuous counterpart of Fig. 3. Fig. 4 includes a group of 14 attractors, shown in Table 5, which appeared in the perturbation analysis but that were not found doing a random search. Note that all these attractors have at least one variable with a value of 0.5, thus lacking a counterpart in the discrete model. The explanation for the inability of finding these novel attractors by using a large random sampling of initial states is that these attractors have relatively small basins, thus having a very small probability of being found by chance. To obtain an approximation of the relative size for the basins of attraction, we performed a boundary analysis. The results, in Table 6, show that the basins of the 10 attractors in Table 4 span for larger regions of the state space than the basins of the 14 newly found attractors. In fact, ten of the latter basins span for only a single point in one dimension.

An important aspect of the methodology used here to implement the FOS-GRN as a continuous dynamical system, is that the differential equations have two parameters (see Section 4). Since there is no experimental data to fit the values of such parameters, we used a series of default values as it has been done before (Di Cara et al., 2007; Mendoza and Xenarios, 2006). Nevertheless, it is instructive to know the dependency of the number and position of the fixed point attractors on the values used for the parameters. We solved the continuous model for 10,000 random initial conditions, but this time values for the decaying rate (parameter γ) took random values in the interval [1,1.2]. Table 7 shows that the system still recovers ten fixed point attractors, which are very close in position to those shown in Table 4, but note the large dispersion around the attractors. Therefore, the effect of using random decay rates had an effect similar to introducing noise to the system, slightly altering the location of the attractors. Also, once again none of the attractors with small basins was found with a random sampling.

As with the discrete model, not all the possible pathways shown in Fig. 4 are actually seen during flower development. Fig. 5 is a subgraph of Fig. 4, and includes only those pathways that agree with the qualitative data already published. First, note that unlike the discrete model, there are several pathways leading from an inflorescence state to the sepal attractor. Notably, while

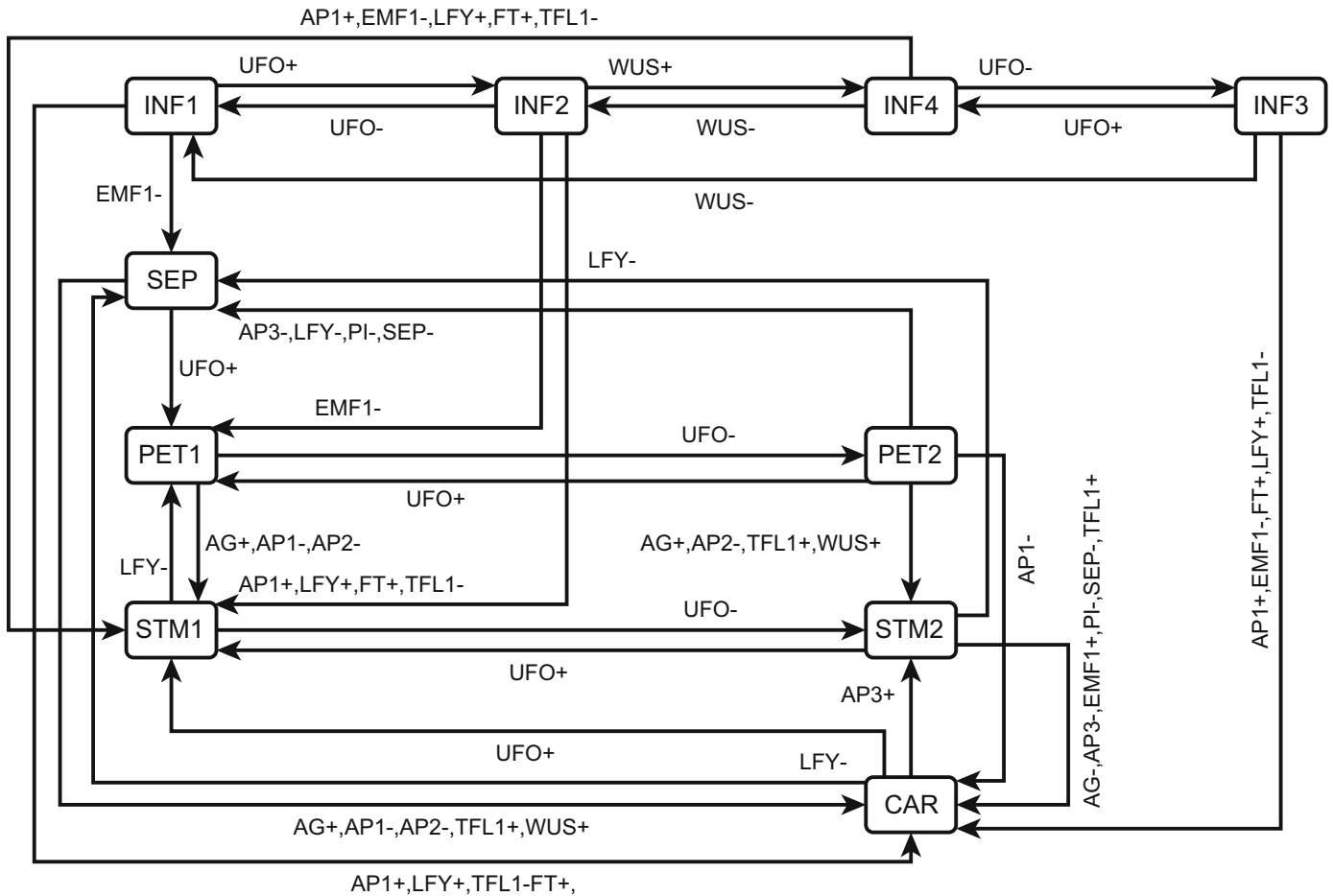


Fig. 3. Complete fate map of the discrete model. Legends are as in Fig. 2.

Table 4
The fixed point attractors of the continuous FOS-GRN model.^a

	INF1	INF2	INF3	INF4	SEP	PET1	PET2	STM1	STM2	CAR
AG	1.3E-9	1.3E-9	1.2E-9	1.2E-9	1.1E-9	1.1E-9	9.6E-10	1.0E+0	1.0E+0	1.0E+0
AP1	1.0E-9	1.0E-9	1.1E-9	1.1E-9	1.0E+0	1.0E+0	1.0E+0	3.1E-9	2.0E-9	3.4E-9
AP2	1.2E-9	1.2E-9	1.2E-9	1.2E-9	1.0E+0	1.0E+0	1.0E+0	1.0E+0	1.0E+0	1.0E+0
AP3	1.2E-9	1.3E-9	1.1E-9	1.2E-9	9.5E-10	1.0E+0	1.0E+0	1.0E+0	1.0E+0	8.6E-10
EMF1	1.0E+0	1.0E+0	1.0E+0	1.0E+0	2.1E-9	2.0E-9	1.5E-9	1.3E-9	9.9E-10	1.4E-9
FT	1.1E-9	1.1E-9	1.1E-9	1.1E-9	1.0E+0	1.0E+0	1.0E+0	1.0E+0	1.0E+0	1.0E+0
FUL	1.2E-9	1.2E-9	1.2E-9	1.2E-9	1.81E-9	1.8E-9	1.5E-9	1.0E+0	1.0E+0	1.0E+0
LFY	8.6E-10	8.7E-10	8.4E-10	8.3E-10	1.0E+0	1.0E+0	1.0E+0	1.0E+0	1.0E+0	1.0E+0
PI	1.2E-9	1.2E-9	1.2E-9	1.2E-9	1.3E-9	1.0E+0	1.0E+0	1.0E+0	1.0E+0	1.0E+0
SEP	1.2E-9	1.2E-9	1.1E-9	1.0E-9	1.0E+0	1.0E+0	1.0E+0	1.0E+0	1.0E+0	1.0E+0
TFL1	1.0E+0	1.0E+0	1.0E+0	1.0E+0	9.4E-10	9.2E-10	7.8E-10	1.0E-9	1.0E-9	1.1E-9
UFO	5.4E-10	1.0E+0	5.2E-10	1.0E+0	5.2E-10	1.0E+0	5.2E-10	1.0E+0	5.3E-10	5.2E-10
WUS	5.8E-10	5.9E-10	1.0E+0	1.0E+0	5.5E-10	5.5E-10	5.5E-10	3.5E-9	2.2E-9	3.9E-9

^a Values are averages of 50,000 runs (see Section 4). In all cases the associated standard deviations are smaller than 1.00E-9.

in the discrete model the inactivation of *EMF1* was found to be the sole signal promoting a transition from an inflorescence to sepals, the continuous models reveal that this process requires the coordination of a set of signals. Specifically, in the continuous model the appearance of sepals involve the inactivation *EMF1* and of *TFL1*, as well as the activation of *AP1* and *LFY*. These results are in perfect agreement with the established role of *EMF1* and *TFL1* as floral inhibitors and of *AP1* and *LFY* as floral promoters (Shannon and Meeks-Wagner, 1993). During the floral transition, therefore, the continuous model agrees with a larger set of qualitative experimental data than the discrete model.

The discrete and continuous models have many similarities regarding the signals required for the transitions among floral attractors. The transition from sepals to petals requires the activation of *UFO* in both models, while the continuous model also shows the possible participation of the activation of *AP3*, an aspect that is in agreement with the available experimental information, as discussed above (Chae et al., 2008). Both models coincide that the activation of *AG* and *WUS* is sufficient for the transition from petals to stamens, and that the transition from stamens to carpels can be attained by an inactivation of *AP3*. Furthermore, it is evident from studying Fig. 5 that *WUS* and *UFO* play a key role during

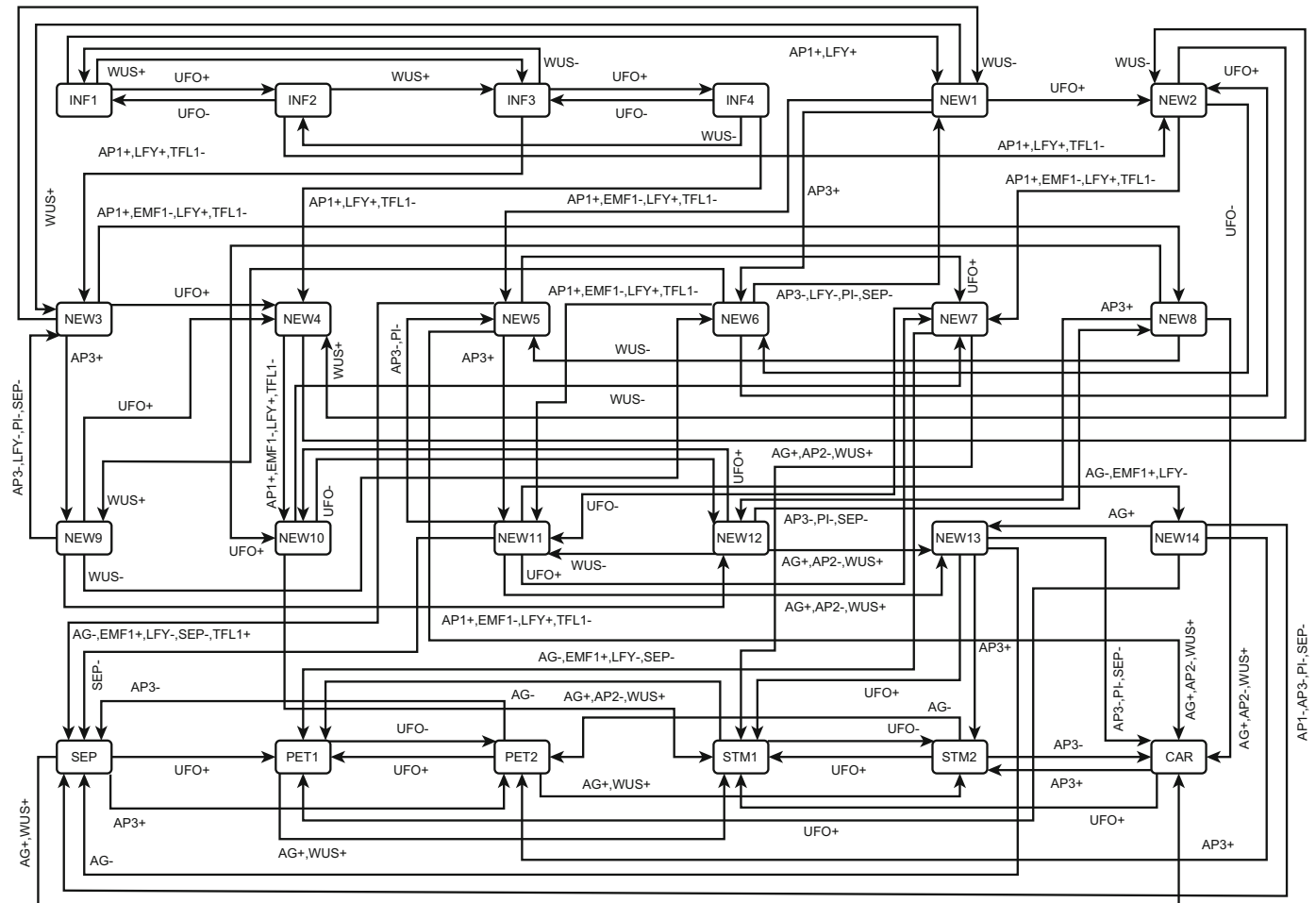


Fig. 4. Complete fate map of the continuous model. Legends are as in Fig. 2.

Table 5

Fixed point attractors of the continuous systems not found in the random search.

	NEW1	NEW2	NEW3	NEW4	NEW5	NEW6	NEW7	NEW8	NEW9	NEW10	NEW11	NEW12	NEW13	NEW14
AG	0.5	0.5	0.5	0.5	0.5	0.5	0.5	0.5	0.5	0.5	0.5	0.5	1	0
AP1	0.5	0.5	0.5	0.5	0.5	0.5	0.5	0.5	0.5	0.5	0.5	0.5	0	1
AP2	0.5	0.5	0.5	0.5	1	0.5	1	1	0.5	1	1	1	1	1
AP3	0	0.5	0	0.5	0	0.5	1	0	0.5	1	0.5	0.5	0.5	0.5
EMF1	0.5	0.5	0.5	0.5	0	0.5	0	0	0.5	0	0	0	0	0
FT	0.5	0.5	0.5	0.5	1	0.5	1	1	0.5	1	1	1	1	1
FUL	0.5	0.5	0.5	0.5	0.5	0.5	0.5	0.5	0.5	0.5	0.5	0.5	1	0
LFY	0.5	0.5	0.5	0.5	1	0.5	1	1	0.5	1	1	1	1	1
PI	0.5	0.5	0.5	0.5	0.5	0.5	1	0.5	0.5	1	0.5	0.5	1	0.5
SEP	0.5	0.5	0.5	0.5	1	0.5	1	1	0.5	1	1	1	1	1
TFL1	0.5	0.5	0.5	0.5	0	0.5	0	0	0.5	0	0	0	0	0
UFO	0	1	0	1	0	0	1	0	0	1	0	0	0	0
WUS	0	0	1	0.5	0	0	0	0.5	0.5	0.5	0	0.5	0	0

differentiation since they appear in most pathways. This aspect is in qualitative agreement with the available experimental evidence for *WUS* and *UFO* (Mayer et al., 1998; Samach et al., 1999). It is important to note that the transitions among the floral attractors, if not identical between the two models, are quite similar and both of them are in agreement with the existing experimental evidence.

2.3. Simulation of mutants

Validation of network models requires not only the description of wild type expression patterns, but also of those expression

profiles observed under several mutant backgrounds. We simulated a series of loss and gain of function mutants with both the discrete and continuous versions of the FOS-GRN model. In particular, we simulated the effects of loss-of-function mutations on *AP2*, *AP3* and the gain-of-function mutations on *AP3* and *AG*. These mutants have been modeled previously, and are included here to test the consistency among the present and past versions of the FOS-GRN. The mutants simulated in the present study recovered the same attractors as in the previous versions of the network (Chaos et al., 2006; Espinosa-Soto et al., 2004).

The *ap2* loss of function mutation does not have sepals or petals, while stamens and carpels are structurally similar to wild

Table 6
Boundary analysis for the basins of attraction.^a

	AG	AP1	AP2	AP3	EMF1	FT	FUL	LFY	PI	SEP	TFL1	UFO	WUS
inf1	[0,1]	[0,1]	[0,1]	[0,1]	[0,1]	[0,1]	[0,1]	[0,1]	[0,1]	[0,1]	[0,1]	[0,0.5]	[0,0.5]
inf2	[0,1]	[0,1]	[0,1]	[0,1]	[0,1]	[0,1]	[0,1]	[0,1]	[0,1]	[0,1]	[0,1]	(0.5,1]	[0,0.5]
inf3	[0,1]	[0,1]	[0,1]	[0,1]	[0,1]	[0,1]	[0,1]	[0,1]	[0,1]	[0,1]	(0,1]	[0,0.5]	(0.5,1]
inf4	[0,1]	[0,1]	[0,1]	[0,1]	[0,1]	[0,1]	[0,1]	[0,1]	[0,1]	[0,1]	[0,1]	(0.5,1]	(0.5,1]
sep	[0,0.5]	[0,1]	[0,1]	[0,1]	[0,1]	[0,1]	[0,1]	[0,1]	[0,1]	[0,1]	[0,1]	[0,0.5]	[0,0.5]
pet1	[0,0.5]	[0,1]	[0,1]	[0,1]	[0,1]	[0,1]	[0,1]	[0,1]	[0,1]	[0,1]	[0,1]	(0.5,1]	[0,0.5]
pet2	[0,0.5]	[0,1]	[0,1]	(0.5,1]	[0,1]	[0,1]	[0,1]	[0,1]	[0,1]	[0,1]	[0,1]	[0,0.5]	[0,0.5]
st1	(0.5,1]	[0,1]	[0,1]	[0,1]	[0,1]	[0,1]	[0,1]	[0,1]	[0,1]	[0,1]	[0,1]	(0.5,1]	[0,1]
st2	(0.5,1]	[0,1]	[0,1]	(0.5,1]	[0,1]	[0,1]	[0,1]	[0,1]	[0,1]	[0,1]	[0,1]	[0,0.5]	[0,1]
car	(0.5,1]	[0,1]	[0,1]	[0,0.5]	[0,1]	[0,1]	[0,1]	[0,1]	[0,1]	[0,1]	[0,1]	[0,0.5]	[0,1]
new1	[0,1]	[0,0.5]	[0,1]	[0,0.5]	[0.5,1]	[0,1]	[0,1]	[0,0.5]	[0,1]	[0,1]	[0.5,1]	[0,0.5]	[0,0.5]
new2	[0,1]	[0,0.5]	[0,1]	[0,1]	[0.5,1]	[0,1]	[0,1]	[0,0.5]	[0,1]	[0,1]	[0.5,1]	(0.5,1]	[0,0.5]
new3	[0,1]	[0,0.5]	[0,1]	[0,0.5]	[0.5,1]	[0,1]	[0,1]	[0,0.5]	[0,1]	[0,1]	[0.5,1]	[0,0.5]	[0.5,1]
new4	[0,1]	[0,0.5]	[0,1]	[0,1]	[0.5,1]	[0,1]	[0,1]	[0,0.5]	[0,1]	[0,1]	[0.5,1]	(0.5,1]	[0.5,1]
new5	0.5	[0,1]	[0.5,1]	[0,0.5]	[0,0.5]	[0,1]	[0,1]	[0.5,1]	[0,1]	[0.5,1]	[0,1]	[0,0.5]	[0,0.5]
new6	[0,1]	[0,0.5]	[0,1]	[0.5,1]	[0.5,1]	[0,1]	[0,1]	0.5	[0.5,1]	[0.5,1]	[0.5,1]	[0,0.5]	[0,0.5]
new7	0.5	[0,1]	[0.5,1]	[0,1]	[0,0.5]	[0,1]	[0,1]	[0.5,1]	[0,1]	[0.5,1]	[0,1]	(0.5,1]	[0,0.5]
new8	[0,0.5]	[0,1]	[0.5,1]	[0,0.5]	[0,1]	[0,1]	[0,1]	[0.5,1]	[0,1]	[0,1]	[0,1]	[0,0.5]	0.5
new9	[0,1]	[0,0.5]	[0,1]	[0.5,1]	[0.5,1]	[0,1]	[0,1]	0.5	[0.5,1]	[0.5,1]	[0.5,1]	[0,0.5]	[0.5,1]
new10	[0,0.5]	[0,1]	[0.5,1]	[0,1]	[0,1]	[0,1]	[0,1]	[0,1]	[0,1]	[0,1]	[0,1]	(0.5,1]	0.5
new11	0.5	[0,1]	[0.5,1]	[0.5,1]	[0,0.5]	[0,1]	[0,1]	[0.5,1]	[0.5,1]	[0.5,1]	[0,1]	[0,0.5]	[0,0.5]
new12	[0,0.5]	[0,1]	[0.5,1]	[0.5,1]	[0,1]	[0,1]	[0,1]	[0,1]	[0.5,1]	[0.5,1]	[0,1]	[0,0.5]	0.5
new13	(0.5,1]	[0,1]	[0,1]	0.5	[0,1]	[0,1]	[0,1]	[0,1]	[0.5,1]	[0.5,1]	[0,1]	[0,0.5]	[0,1]
new14	[0,0.5]	[0.5,1]	[0,1]	0.5	[0,1]	[0,1]	[0,1]	[0,1]	[0.5,1]	[0.5,1]	[0,1]	[0,0.5]	[0,0.5]

^a Intervals in each dimension covered by the corresponding basin of attraction.

type organs but increased in number (Riechmann and Meyerowitz, 1997). Our simulations agree with the experimental data. Table 8 shows that the FOS-GRN *ap2* mutant loses the attractors corresponding to sepals and petals. Moreover, the basin of attraction of stamens and carpels notably increases.

Null mutants in the *AP3* gene are characterized by altered organ specification in whorls 2 and 3. Specifically, petals are transformed into sepals and the stamens into carpels (Bowman et al., 1989; Jack et al., 1992), though sometimes intermediate structures known as sepaloids and staminoids appear (Riechmann and Meyerowitz, 1997). In agreement with this experimental evidence, the simulated *ap3* mutant lacks both petal and stamen attractors, as shown in Table 9. Contrary to the *ap2* mutant model, the attractors do not disappear totally, but are replaced by fixed point attractor that can be easily interpreted as sepaloid and staminoids organs due to their activation patterns. Once again, the basins of attraction of carpels and sepals are increased in size when compared against the wild type background, in agreement with the experimental data.

We then modeled the effect of the constitutive expression of *AP3*. Experimentally, the constitutive expression of *AP3* with the use of the CaMV35S promoter leads to the development of petals instead of sepals in the first floral whorl, and of stamens instead of carpels in the fourth whorl (Jack et al., 1994). Accordingly, the simulation of this gain of function mutant yielded configurations without the attractors corresponding to either sepals or carpels, as shown in Table 10.

Finally, the experimental over-expression of *AG* results in flowers that do not present sepals or petals. Instead, organs with some characteristics of carpels and stamens appear on the first and second whorls (Riechmann and Meyerowitz, 1997). Table 11 shows the result of simulating the overexpression of *AG*. Both the discrete and continuous models correctly lack the attractors corresponding to sepals and petals.

3. Discussion

We updated the *A. thaliana* flower organ specification gene regulatory network, adding three interactions and modifying two

logical rules. The present version of the FOS-GRN, when modeled as a discrete dynamical system, retains the same ten attractors of the previous published model (Chaos et al., 2006), showing that such behavior is determined to a large extent by the topology of the network. Furthermore, the simulation of two loss-of-function and two gain-of-function mutants also agree with published experimental data and previous versions of the model. While the present version of the FOS-GRN behaves as the previous versions of the model, it incorporates new published experimental evidence, making it more biologically accurate than its predecessors.

We also presented a continuous version of the FOS-GRN. This kind of modeling was hampered due to a lack of enough quantitative information regarding the expression levels of the involved genes, thus impeding parameter fitting against experimental data. To circumvent this obstacle, we decided to develop a qualitative continuous model, using a modification of the standardized qualitative dynamical method (Mendoza and Xenarios, 2006), which allows the translation of given gene regulatory network into a continuous dynamical system. The modification used here consists in the inclusion of a continuous version of the logical rules describing the response of nodes directly into the differential equations. This characteristic, added to the choice of numerical values for the parameters (see Section 4), ensures a direct comparison between the discrete and continuous versions of the FOS-GRN presented in this study. Furthermore, the use of the standardized qualitative dynamical method creates the opportunity of doing a sensitive analysis, exploring the effect of modifying the form of the response curve on the number, type and location of the recovered attractors.

In a previous approach, the FOS-GRN was modeled with the use of piecewise-linear Glass dynamics (Álvarez-Buylla et al., 2008). Such implementation requires the association of each node with two variables, one continuous variable to represent the level of expression of a given gene, and one binary variable to represent the state of expression of the same gene. Such duplicity has the drawback that there are infinitely many continuous network states corresponding to one discrete network state. Furthermore, two different initial continuous states that correspond to the same discrete state may end in different attractors. These are

Table 7
Attractors of the continuous model with random values of γ^a .

	INF1		INF2		INF3		INF4	
	AVERAGE	ST. DEV.	AVERAGE	ST. DEV.	AVERAGE	ST. DEV.	AVERAGE	ST. DEV.
AG	6.29E-09	1.16E-08	6.82E-09	1.13E-08	6.83E-09	1.10E-08	6.87E-09	1.29E-08
AP1	7.23E-09	1.15E-08	6.11E-09	1.11E-08	6.56E-09	1.19E-08	7.70E-09	1.19E-08
AP2	1.05E-09	4.00E-09	7.42E-10	3.33E-09	7.07E-10	2.86E-09	1.02E-09	4.26E-09
AP3	1.22E-23	2.80E-23	7.21E-18	8.62E-18	7.23E-24	1.98E-23	8.19E-18	9.61E-18
EMF1	9.18E-01	4.88E-02	9.11E-01	4.69E-02	9.12E-01	4.80E-02	9.18E-01	4.83E-02
FT	5.28E-10	2.15E-09	6.01E-10	2.30E-09	1.01E-09	3.61E-09	6.43E-10	2.48E-09
FUL	7.22E-09	1.15E-08	6.16E-09	1.12E-08	6.51E-09	1.17E-08	7.82E-09	1.22E-08
LFY	1.17E-08	1.40E-08	1.14E-08	1.36E-08	1.18E-08	1.39E-08	1.29E-08	1.50E-08
PI	3.88E-18	7.13E-18	4.23E-18	7.07E-18	4.21E-18	6.81E-18	4.29E-18	8.05E-18
SEP	7.37E-18	8.81E-18	7.19E-18	8.59E-18	7.47E-18	8.74E-18	8.18E-18	9.56E-18
TFL1	9.09E-01	4.69E-02	9.17E-01	4.81E-02	9.15E-01	4.77E-02	9.08E-01	4.80E-02
UFO	4.18E-24	1.07E-23	9.10E-01	4.71E-02	4.22E-24	9.86E-24	9.17E-01	4.70E-02
WUS	5.95E-24	1.47E-23	4.47E-24	1.17E-23	9.13E-01	4.72E-02	9.13E-01	4.72E-02
	SEP		PET1		PET2		STM1	
	AVERAGE	ST. DEV.	AVERAGE	ST. DEV.	AVERAGE	ST. DEV.	AVERAGE	ST. DEV.
AG	6.80E-09	1.17E-08	7.41E-09	1.27E-08	7.35E-09	1.30E-08	9.12E-01	4.76E-02
AP1	9.11E-01	4.85E-02	9.11E-01	4.91E-02	9.15E-01	4.72E-02	7.07E-09	1.17E-08
AP2	9.13E-01	4.72E-02	9.12E-01	4.79E-02	9.14E-01	4.82E-02	9.12E-01	4.75E-02
AP3	8.53E-24	2.04E-23	9.12E-01	4.84E-02	9.18E-01	4.71E-02	9.12E-01	4.82E-02
EMF1	7.41E-10	2.69E-09	9.67E-10	3.77E-09	8.16E-10	2.76E-09	7.60E-10	2.99E-09
FT	9.16E-01	4.76E-02	9.11E-01	4.85E-02	9.13E-01	4.68E-02	9.10E-01	4.81E-02
FUL	7.31E-09	1.18E-08	7.85E-09	1.28E-08	6.27E-09	1.14E-08	9.11E-01	4.81E-02
LFY	9.11E-01	4.76E-02	9.11E-01	4.81E-02	9.17E-01	4.70E-02	9.11E-01	4.73E-02
PI	4.31E-18	7.46E-18	9.12E-01	4.86E-02	9.13E-01	4.82E-02	9.11E-01	4.80E-02
SEP	9.10E-01	4.68E-02	9.12E-01	4.78E-02	9.04E-01	4.67E-02	9.11E-01	4.82E-02
TFL1	4.67E-19	1.69E-18	6.03E-19	2.33E-18	5.09E-19	1.69E-18	4.80E-19	1.89E-18
UFO	4.68E-24	1.07E-23	9.12E-01	4.85E-02	4.41E-24	1.20E-23	9.12E-01	4.80E-02
WUS	4.99E-24	1.21E-23	5.05E-24	1.21E-23	3.04E-24	6.95E-24	2.89E-23	7.79E-23
	STM2		CAR					
	AVERAGE	ST. DEV.	AVERAGE	ST. DEV.				
AG	9.10E-01	4.86E-02	9.13E-01	4.84E-02				
AP1	7.71E-09	1.23E-08	6.90E-09	1.15E-08				
AP2	9.12E-01	4.98E-02	9.12E-01	4.70E-02				
AP3	9.13E-01	4.75E-02	8.19E-24	2.10E-23				
EMF1	7.79E-10	3.35E-09	6.93E-10	2.98E-09				
FT	9.07E-01	4.78E-02	9.12E-01	4.81E-02				
FUL	9.09E-01	4.87E-02	9.12E-01	4.77E-02				
LFY	9.13E-01	4.81E-02	9.11E-01	4.82E-02				
PI	9.09E-01	4.72E-02	9.13E-01	4.76E-02				
SEP	9.13E-01	4.82E-02	9.12E-01	4.73E-02				
TFL1	4.91E-19	2.11E-18	4.41E-19	1.90E-18				
UFO	4.75E-24	1.19E-23	5.13E-24	1.24E-23				
WUS	2.08E-23	5.20E-23	3.43E-23	9.90E-23				

^a Average and standard deviation for 10,000 runs.

unnecessary complications that are not present in our current model. In our present implementation, one continuous variable describes the state of activation of a node. Moreover, we selected parametric values so as to obtain response curves very similar to step functions, and thus making a direct comparison between the discrete and continuous versions of our current version of the FOS-GRN.

The first analysis we performed on the continuous FOS-GRN model was to find its steady states. We found 24 fixed point attractors, ten of which correspond exactly to those found in the discrete version of the model, having a clear biological interpretation. The other 14 attractors contain intermediate values in some of the variables representing gene activity; hence they could not possibly have a counterpart in the discrete model. We could not find published experimental data to interpret the biological meaning of these attractors, unique of the continuous model. A possible reason for this lack of information may be the transient

expression of a subset of the modeled genes, due to the effect of genes and/or regulatory interactions not incorporated to our model. For example, epigenetic changes such as chromatin associated phenomena might account for transient expression of some genes (Más, 2008). These changes in chromatin structure have been associated with the control of floral induction (Farrona et al., 2008). Noteworthy, some genes included in the FOS-GRN such as *FT*, *AG*, *AP3*, *PI* and *SEP3* have been related to the assembly platform for repressive complexes at the chromatin level (Barrero et al., 2007; Farrona et al., 2008). Another, non-exclusive possibility to account for the relatively short lifespan of certain signals is the post-translational modification of gene products (Más, 2008). Finally, yet another possible explanation for the lack of experimental evidence on the 14 attractors exclusive of the continuous model is the relatively small size of their basins. Indeed, since attractors with small basins have a diminished capacity of absorbing perturbations, it is reasonable to expect that they also

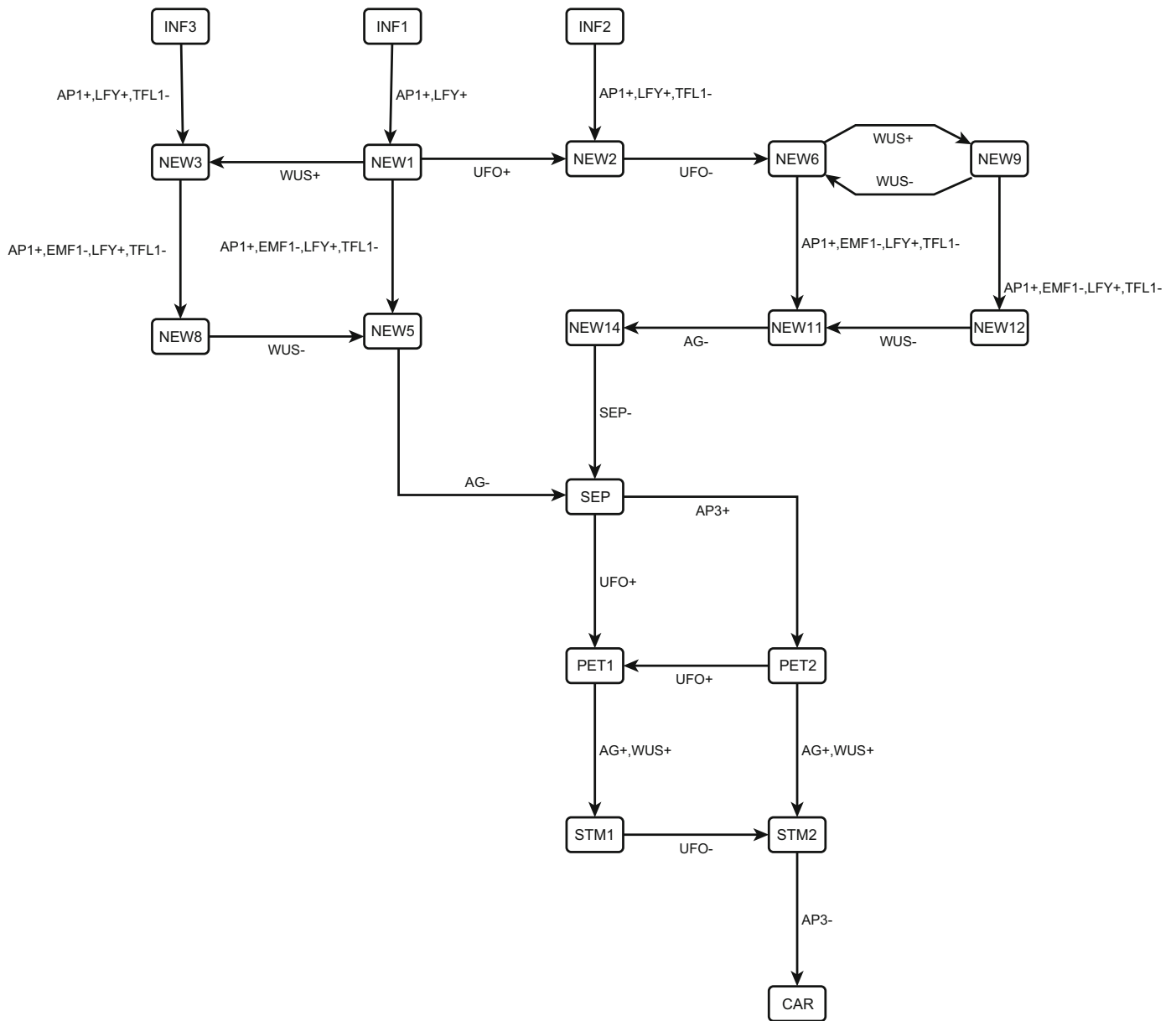


Fig. 5. Biologically relevant developmental routes of the continuous model. Legends are as in Fig. 2.

Table 8

Attractors and relative size of their basins for the simulated *ap2* loss of function mutant.

Attractor	Discrete model (%)	Continuous model (%)
INF1	1.95	4.9
INF2	1.95	4.7
INF3	1.17	4.7
INF4	1.17	3.9
STM1	46.87	41.22
STM2	1.02	8.67
CAR	45.84	32.52

Table 9

Attractors and relative size of their basins for the simulated *ap3* loss of function mutant.^a

Attractor	Discrete model (%)	Continuous model (%)
INF1	1.66	4.98
INF2	1.66	4.79
INF3	0.87	4.09
INF4	0.87	3.98
SEP	10.05	13.06
SEP-like	10.05	12.87
CAR	37.4	28.2
CAR-like	37.4	28.2

^a SEP-like=sepaloid attractor, CAR-like=carpeloid attractor.

have a short life span, since molecular noise might eventually move the system out of the small basin into a large one.

The ten attractors with a clear biological interpretation are recovered in the continuous version of the FOS-GRN not only with the use of default parameters. Assigning random values for the decaying rate in all differential equations, the system still

converges to these ten fixed points. Their location, however, vary slightly among runs. Varying γ , thus, was equivalent in our system to introducing an amount of noise to the system, as revealed by the considerable increase in the standard deviation for the

Table 10

Attractors and relative size of their basins for the simulated 35S::AP3 gain of function mutant.

Attractor	Discrete model (%)	Continuous model (%)
INF1	1.36	5.18
INF2	1.36	5.1
INF3	0.72	4.22
INF4	0.72	4.09
PET1	8.24	12.31
PET2	8.24	13.12
STM1	30.64	12.31
STM2	30.64	28.24

Table 11

Attractors and relative size of their basins for the simulated 35S::AG gain of function mutant.

Attractor	Discrete model (%)	Continuous model (%)
INF1	1.66	6.17
INF2	1.66	6.15
INF3	0.87	4.56
INF4	0.87	4.5
STM1	1.75	8.91
STM2	47.46	39.43
CAR	45.46	30.28

location of the fixed points when compared against the version will identical decay rates for all nodes. This capacity of the system to conserve at least the biologically relevant attractors when varying parameter γ is another aspect of the robustness of the continuous FOS-GRN model. We did not explore if the 14 attractors not present in the discrete model are still conserved in the noisy dynamical system, or if the transitions between attractors is conserved. It is reasonable to suspect that these properties will be altered, though, due to the relative small size of the basins of the novel attractors. Nonetheless, this is a property that will be addressed in a future study with a systematic variation of parameters.

While the biological meaning of the attractors with relative small basins is still under study, their location suggests that could have a role in canalizing the transition from an inflorescence to a floral primordia, specifically to sepal primordia cell types. It is very likely that additional genes and/or other regulatory mechanisms important for such transitions during early flower development are still uncovered. The reason is that these intermediate attractors create several routes, most of them involving the inhibition of the known floral repressors as well as the activation of the known floral inductors. The existence of several routes from inflorescence meristems to flower meristems and primordial floral organ cells, varying primarily in the order of activation of key genes, ensure the appearance of the first floral organs, e.g. sepals, regardless the possible disruption or modification of gene activation order. This property thus gives a high probability of obtaining the correct transitions among attractors, regardless of possible environmental or genetic noise. From this point of view, our results are complementary to the modeling of the *Arabidopsis* flowering as a stochastic system (Álvarez-Buylla et al., 2008), where relatively low levels of intrinsic noise drive the system through the correct sequence of gene activations. In our deterministic system, the existence of multiple paths creates an additional mechanism by which extrinsic noise can be absorbed by canalizing the possible responses of the network, conferring robustness to this differentiation process (Bäurle and Dean, 2006; Parcy, 2005).

The discrete and continuous version of the FOS-GRN coincides on the establishment of the inflorescence and floral attractors

under a wild type genetic background. Furthermore, they also have an identical and correct response on the simulation of certain mutants. The identity among the several versions and implementations of the FOS-GRN confirms that the global behavior of the network is largely determined by its topology, rather than by the particularities of the mathematical framework used for its modeling (Chaos et al., 2006).

The simulation of cell differentiation by means of Boolean models has been criticized because of its apparent oversimplification of the observed complexity of the regulation of gene activation. Our implementation of the latest version of the FOS-GRN both as a continuous and a dynamical system shows that they behave quite similarly. Such results gives a strong support that the dynamical behavior of a regulatory network model to a large extent depends on the topology of the network, as it has been shown for other biological systems (Albert and Othmer, 2003; Di Cara et al., 2007; Mendoza, 2006; Mendoza and Xenarios, 2006; von Dassow et al., 2000).

4. Methods

4.1. Updated FOS-GRN

Fig. 1 shows the genetic regulatory network that controls the determination of floral organ primordial cell types; its topology was inferred from a thorough review of published genetic and molecular experiments. This network has been modified and updated several times (Chaos et al., 2006; Espinosa-Soto et al., 2004; Mendoza and Álvarez-Buylla, 1998). In this section we explain the information used to update the FOS-GRN in this study. The resulting logical rules describing the Boolean version of the network are shown in Table 1.

Recently, it has been shown that *EMF1* down-regulates *AG* (Calonje et al., 2008). Using ChIP experiments, *EMF1* was found to recognize regulatory sites located in the promoter and second intron of *AG*. Furthermore, *EMF1* interfered with the transcription of *AG* by RNA polymerase II and T7 RNA polymerase *in vitro* (Calonje et al., 2008). This information was incorporated in the *AG* logical rule by turning *AG* off whenever *EMF1* is present. Otherwise, when *EMF1* is zero, *AG* is turned off by *TFL1* or *AP2*, except in three cases: (1) when both *LFY* and *WUS* are on, (2) when *AG*, *SEP1-3* and *LFY* are on and *TFL1* is off and (3) when *LFY* is on and *AP1* or *AP2* are off.

AP3 and *PI* are both able to down-regulate *AP1* (Sundström et al., 2006). On the one hand, ChIP experiments showed that the *PI* protein binds to target sequences in the *AP1* promoter, eventually leading to decreased expression of *AP1*. And on the other hand, *AP1* transcript levels are significantly elevated in *ap3-3* mutant plants when compared against both *WT* and 35S::AP3 plants (Sundström et al., 2006). As a result, the *AP1* logical rule was modified in such a way that when *AP3* or *PI* is on, *AP1* is on whenever *AG* is off but *FT* or *LFY* are on.

4.2. The discrete model

In the discrete approach each gene in the network is represented by a Boolean variable x that takes the value of 0 or 1 to represent its active or inactive state of expression, respectively. The activation state of the whole network is then represented by a vector with the set of Boolean variables $\{x_1, x_2, \dots, x_n\}$, where x_i is the state of expression of the i th gene.

The state of expression of each gene changes in discrete time steps according to $x_i(t+1) = F_i(x_1(t), x_2(t), \dots, x_n(t))$, where $\{x_1(t), x_2(t), \dots, x_n(t)\}$ is the state of regulators of gene x_i at time t ,

and F_i is a Boolean function, also called a logical rule, determining the state of gene x_i at the next time step. Each gene in the network has its own associated Boolean function, see Table 1.

Since the number of states of the network is finite, specifically 2^N , the dynamics of the network can be tested for all possible initial conditions. We did such analysis using the software package Atalia developed by Alvaro Chaos in Álvarez-Buylla's laboratory.

4.3. The continuous model

The standardized qualitative dynamical systems method (Mendoza and Xenarios, 2006) was developed to automatically translate the topology of a discrete regulatory network into a continuous dynamical system and study its behavior. In its original implementation, the methodology assigns a set of default values to several parameters, so as to make a fully automated analysis. However, such methodology was not appropriate in its

original form for the present study; the reason is that the approach assumes that a negative interaction is always stronger than any activation or group of simultaneous activations. This is not the case in our present FOS-GRN model. For example, the logical rule of *AP1* (Table 1) implies that the activation of *LFY* is stronger than the inhibition of *TFL1*.

We decided to modify the standardized qualitative dynamical systems approach so as to be able to include specific logical rules that differed from the default rules, as in the case of *AP1*, *WUS*, *AG* and *TFL1*. As a result, the continuous system is modeled as a series of coupled ordinary differential equations, describing the activation of node x_i with an equation of the form:

$$\frac{dx_i}{dt} = \frac{-e^{0.5h} + e^{-h*(\omega_i-0.5)}}{(1-e^{0.5h})*(e^{-h*(\omega_i-0.5)})} - \gamma_i x_i$$

The right-hand side of the equation has two parts: a sigmoid function to account for the rate of production and a linear term to account for the decay of x_i . The former includes the parameter h

Table 12
Equations describing the continuous FOS-GRN model.

$\frac{dAG}{dt} = \frac{-e^{25} + e^{-50(\omega_{AG}-0.5)}}{(1-e^{25})(1+e^{-50(\omega_{AG}-0.5)})} - AG$
$\frac{dAP1}{dt} = \frac{-e^{25} + e^{-50(\omega_{AP1}-0.5)}}{(1-e^{25})(1+e^{-50(\omega_{AP1}-0.5)})} - AP1$
$\frac{dAP2}{dt} = \frac{-e^{25} + e^{-50(\omega_{AP2}-0.5)}}{(1-e^{25})(1+e^{-50(\omega_{AP2}-0.5)})} - AP2$
$\frac{dAP3}{dt} = \frac{-e^{25} + e^{-50*(\omega_{AP3}-0.5)}}{(1-e^{25})*(1+e^{-50*(\omega_{AP3}-0.5)})} - AP3$
$\frac{dEMF1}{dt} = \frac{-e^{25} + e^{-50*(\omega_{EMF1}-0.5)}}{(1-e^{25})*(1+e^{-50*(\omega_{EMF1}-0.5)})} - EMF1$
$\frac{dFT}{dt} = \frac{-e^{25} + e^{-50*(\omega_{FT}-0.5)}}{(1-e^{25})*(1+e^{-50*(\omega_{FT}-0.5)})} - FT$
$\frac{dFUL}{dt} = \frac{-e^{25} + e^{-50*(\omega_{FUL}-0.5)}}{(1-e^{25})*(1+e^{-50*(\omega_{FUL}-0.5)})} - FULL$
$\frac{dLFY}{dt} = \frac{-e^{25} + e^{-50*(\omega_{LFY}-0.5)}}{(1-e^{25})*(1+e^{-50*(\omega_{LFY}-0.5)})} - LFY$
$\frac{dPI}{dt} = \frac{-e^{25} + e^{-50*(\omega_{PI}-0.5)}}{(1-e^{25})*(1+e^{-50*(\omega_{PI}-0.5)})} - PI$
$\frac{dSEP}{dt} = \frac{-e^{25} + e^{-50*(\omega_{SEP}-0.5)}}{(1-e^{25})*(1+e^{-50*(\omega_{SEP}-0.5)})} - SEP$
$\frac{dTFL1}{dt} = \frac{-e^{25} + e^{-50*(\omega_{TFL1}-0.5)}}{(1-e^{25})*(1+e^{-50*(\omega_{TFL1}-0.5)})} - TFL1$
$\frac{dUFO}{dt} = \frac{-e^{25} + e^{-50*(\omega_{UFO}-0.5)}}{(1-e^{25})*(1+e^{-50*(\omega_{UFO}-0.5)})} - UFO$
$\frac{dWUS}{dt} = \frac{-e^{25} + e^{-50*(\omega_{WUS}-0.5)}}{(1-e^{25})*(1+e^{-50*(\omega_{WUS}-0.5)})} - WUS$
$\omega_{AG} = \max(\min(1-EMF1, 1-AP2, 1-TFL1), \min(1-EMF1, 1-AP2, UFO), \min(1-EMF1, 1-AP2, LFY), \min(1-EMF1, 1-TFL1, LFY, \min(AG, SEP)), \min(1-EMF1, \min(LFY, WUS)))$
$\omega_{AP1} = \max(\min(1-AG, 1-TFL1), \min(FT, LFY, 1-AG), \min(FT, 1-AG, 1-PI), \min(LFY, 1-AG, 1-PI), \min(FT, 1-AG, 1-AP3), \min(LFY, 1-AG, 1-AP3))$
$\omega_{AP2} = 1-TFL1$
$\omega_{AP3} = \max(\min(LFY, UFO), \min(PI, SEP, AP3, \max(AG, AP1)))$
$\omega_{EMF1} = 1-LFY$
$\omega_{FT} = 1-EMF1$
$\omega_{FUL} = \min(1-AP1, 1-TFL1)$
$\omega_{LFY} = \max(1-EMF1, 1-TFL1)$
$\omega_{PI} = \max(\min(LFY, \max(AG, AP3)), \min(PI, SEP, AP3, \max(AG, AP1)))$
$\omega_{SEP} = LFY$
$\omega_{TFL1} = \min(1-AP1, \min(EMF1, 1-LFY))$
$\omega_{UFO} = UFO$
$\omega_{WUS} = \min(WUS, \max(1-AG, 1-SEP));$

that determines its gain, and contains the variable ω_i that is the continuous form of the truth table describing the response of node x_i . This sigmoid was constructed so as to pass through the points (0,0), (0.5,0.5) and (1,1) for any positive value of h . For large values of h (e.g. 100 and higher) the curve is very close to a step function; for intermediate values of h (around 50) the function is similar to a logistic curve; and as h approaches 0 the curve is almost a straight line. This characteristic allows the study of the influence of different qualitative response curves on the overall dynamical behavior of the network by changing only one parameter, while at the same time conserving the direct comparison against a Boolean model due to the three fixed points mentioned above.

For the present study we decided to use the values of $h=50$ and $\gamma=1$, resulting in the system of equations shown in Table 12. Our choice of values was intended to have response curves very similar to step functions, thus making a straightforward comparison between the boolean and the discrete versions of the FOS-GRN. The system of equations was solved numerically using the mathematical package octave (<http://www.gnu.org/software/octave/>), starting from a large number of random initial states.

It is important to mention that in our continuous model of the FOS-GRN, *UFO* had to incorporate an inexistent self-activation ($\omega_{UFO}=UFO$ in Table 12). The reason for this feature was to ensure that *UFO* reached either full or null activation levels, thus allowing us to observe the behavior of the whole system under these two possibilities.

4.4. Fate maps

For both the discrete and the continuous model, we perturbed every fixed point attractor by altering all nodes, one at a time. This means that in the discrete model we flipped a node either from its value of 0 to 1 or vice versa. For the continuous model we perturbed the value of each node by 0.5 and 1 units. This is, a node with a state of 0 was moved in one instance to 0.5, and in another to 1. If the node had a value of 0.5, it was perturbed to 0 and 1. Finally, if the original state was 1, then the perturbations changed it to 0 and 0.5.

4.5. Boundary analysis

For each attractor in the continuous model we perturbed the system, one variable at a time and solved the system until it converged to a fixed point. The perturbations were systematically done with the modified variable taking values from 0 to 1 in increments of 0.01 units. Results are presented as the intervals for which a given variable was perturbed while the system was still able to return to its original attractor.

Acknowledgements

The authors want to thank the three anonymous reviewers, whose suggestions were very valuable to make this manuscript suitable for publication. This work was supported in part by the CONACYT Grant APOY-COMPL-2008, no. 89664 to LM.

References

Albert, R., Othmer, H.G., 2003. The topology of the regulatory interactions predicts the expression pattern of the segment polarity genes in *Drosophila melanogaster*. *J. Theor. Biol.* 223, 1–18, doi:10.1016/S0022-5193(03)00035-3.

Álvarez-Buylla, E.R., Benítez, M., Dávila, E.B., Chaos, A., Espinosa-Soto, C., Padilla-Longoria, P., 2007. Gene regulatory network models for plant development. *Curr. Opin. Plant Biol.* 10, 83–91, doi:10.1016/j.pbi.2006.11.008.

Álvarez-Buylla, E.R., Chaos, A., Aldana, M., Benítez, M., Cortes-Poza, Y., Espinosa-Soto, C., Hartasánchez, D.A., Lotto, R.B., Malkin, D., Escalera-Santos, G.J., Padilla-Longoria, P., 2008. Floral morphogenesis: stochastic explorations of a gene network epigenetic landscape. *PLoS One* 3, e3626.

Álvarez-Buylla, E.R., Benítez-Keinrad, M., Corvera-Poiré, A., Chaos, A.C., de Foltera, S., Gamboa de Buen, A., Garay-Arroyo, A., García-Ponce, B., Jaimes-Miranda, F., Pérez-Ruiz, R.V., Piñeyro-Nelson, A., Sánchez-Corrales, Y.E., Flower development. In: *The Arabidopsis Book*. Rockville, MD. American Society of Plant Biologists (Eds.). In press. Available from: <<http://www.aspb.org/publications/arabidopsis/>>.

Barrero, J.M., González-Bayón, R., del Pozo, J.C., Ponce, M.R., Micol, J.L., 2007. INCURVATA2 encodes the catalytic subunit of DNA Polymerase alpha and interacts with genes involved in chromatin-mediated cellular memory in *Arabidopsis thaliana*. *Plant Cell* 19, 2822–2838.

Bäurle, I., Dean, C., 2006. The timing of developmental transitions in plants. *Cell* 125, 655–664.

Benítez, M., Espinosa-Soto, C., Padilla-Longoria, P., Álvarez-Buylla, E.R., 2008. Interlinked nonlinear subnetworks underlie the formation of robust cellular patterns in *Arabidopsis epidermis*: a dynamic spatial model. *BMC Syst. Biol.* 2, 98.

Bowman, J.L., Smyth, D.R., Meyerowitz, E.M., 1989. Genes directing flower development in *Arabidopsis*. *Plant Cell* 1, 37–52.

Calonje, M., Sanchez, R., Chen, L., Sung, Z.R., 2008. EMBRYONIC FLOWER1 participates in polycomb group-mediated AG gene silencing in *Arabidopsis*. *Plant Cell* 20, 277–291.

Chaos, A., Aldana, M., Espinosa-Soto, C., García-Ponce, B., Garay, A., Álvarez-Buylla, E., 2006. From genes to flower patterns and evolution: Dynamic models of gene regulatory networks. *J. Plant Growth Regul.* 25, 278–289.

Chae, E., Tan, Q.K., Hill, T.A., Irish, V.F., 2008. An *Arabidopsis* F-box protein acts as a transcriptional co-factor to regulate floral development. *Development* 135, 1235–1245.

Chen, L., Cheng, J., Castle, L., Sung, Z.R., 1997. EMF genes regulate *Arabidopsis* inflorescence development. *Plant Cell* 9, 2011–2024.

Coen, E.S., Meyerowitz, E.M., 1991. The war of the whorls: genetic interactions controlling flower development. *Nature* 353, 31–37.

Deyholos, M.K., Sieburth, L.E., 2000. Separable whorl-specific expression and negative regulation by enhancer elements within the *AGAMOUS* second intron. *Plant Cell* 12, 1799–1810.

Di Cara, A., Garg, A., De Micheli, G., Xenarios, I., Mendoza, L., 2007. Dynamic simulation of regulatory networks using SQUAD. *BMC Bioinformatics* 8, 462.

Drews, G.N., Bowman, J.L., Meyerowitz, E.M., 1991. Negative regulation of the *Arabidopsis* homeotic gene *AGAMOUS* by the *APETALA2* product. *Cell* 65, 991–1002.

Espinosa-Soto, C., Padilla-Longoria, P., Álvarez-Buylla, E.R., 2004. A gene regulatory network model for cell-fate determination during *Arabidopsis thaliana* flower development that is robust and recovers experimental gene expression profiles. *Plant Cell* 16, 2923–2939.

Farrona, S., Coupland, G., Turck, F., 2008. The impact of chromatin regulation on the floral transition. *Semin. Cell Dev. Biol.* 19, 560–573.

Glass, L., 1975. Classification of biological networks by their qualitative dynamics. *J. Theor. Biol.* 54, 85–107, doi:10.1016/S0022-5193(75)80056-7.

Gómez-Mena, C., de Folter, S., Costa, M.M., Angenent, G.C., Sablowski, R., 2005. Transcriptional program controlled by the floral homeotic gene *AGAMOUS* during early organogenesis. *Development* 132, 429–438.

Gustafson-Brown, C., Savidge, B., Yanofsky, M.F., 1994. Regulation of the *Arabidopsis* floral homeotic gene *APETALA1*. *Cell* 76, 131–143.

Huang, S., Ingber, D.E., 2006. A non-genetic basis for cancer progression and metastasis: self-organizing attractors in cell regulatory networks. *Breast Dis.* 26, 27–54.

Jack, T., Brockman, L.L., Meyerowitz, E.M., 1992. The homeotic gene *APETALA3* of *Arabidopsis thaliana* encodes a MADS box and is expressed in petals and stamens. *Cell* 68, 683–697.

Jack, T., Fox, G.L., Meyerowitz, E.M., 1994. *Arabidopsis* homeotic gene *APETALA3* ectopic expression: transcriptional and posttranscriptional regulation determine floral organ identity. *Cell* 76, 703–716.

Lenhard, M., Bonhart, A., Jürgens, G., Laux, T., 2001. Termination of stem cell maintenance in *Arabidopsis* floral meristems by interactions between *WUSCHEL* and *AGAMOUS*. *Cell* 105, 805–814.

Laufs, P., Coen, E., Kronenberger, J., Traas, J., Doonan, J., 2003. Separable roles of *UFO* during floral development revealed by conditional restoration of gene function. *Development* 130, 785–796.

Li, S., Assmann, S.M., Albert, R., 2006. Predicting essential components of signal transduction networks: a dynamic model of guard cell abscisic acid signaling. *PLoS Biol.* 4, e312.

Liu, Z., Meyerowitz, E.M., 1995. *LEUNIG* regulates *AGAMOUS* expression in *Arabidopsis* flowers. *Development* 121, 975–991.

Más, P., 2008. Circadian clock function in *Arabidopsis thaliana*: time beyond transcription. *Trends Cell Biol.* 18, 273–281.

Mayer, K., Schoof, H., Haecker, A., Lenhard, M., Jürgens, G., Laux, T., 1998. Role of *WUSCHEL* in regulating stem cell fate in the *Arabidopsis* shoot meristem. *Cell* 95, 805–815.

Mendoza, L., 2006. A network model for the control of the differentiation process in *Th* cells. *BioSystems* 84, 101–114, doi:10.1016/j.biosystems.2005.10.004.

Mendoza, L., Álvarez-Buylla, E.R., 1998. Dynamics of the genetic regulatory network of *Arabidopsis thaliana* flower morphogenesis. *J. Theor. Biol.* 193, 307–319, doi:10.1006/jtbi.1998.0701.

- Mendoza, L., Thieffry, D., Álvarez-Buylla, E.R., 1999. Genetic control of flower morphogenesis in *Arabidopsis thaliana*: a logical analysis. *Bioinformatics* 15, 593–606.
- Mendoza, L., Xenarios, I., 2006. A method for the generation of standardized qualitative dynamical systems of regulatory networks. *Theor. Biol. Med. Model.* 3, 13.
- Moon, Y., Chen, L., Pan, R.L., Chang, H., Zhu, T., Maffeo, D.M., Sung, Z.R., 2003. EMF genes maintain vegetative development by repressing the flower program in *Arabidopsis*. *Plant Cell* 15, 681–693.
- Parcy, F., 2005. Flowering: a time for integration. *Int. J. Dev. Biol.* 49, 585–593.
- Riechmann, J.L., Meyerowitz, E.M., 1997. Determination of floral organ identity by *Arabidopsis* MADS domain homeotic proteins AP1, AP3, PI, and AG is independent of their DNA-binding specificity. *Mol. Biol. Cell.* 8, 1243–1259.
- Samach, A., Klenz, J.E., Kohalmi, S.E., Risseuw, E., Haughn, G.W., Crosby, W.L., 1999. The UNUSUAL FLORAL ORGANS gene of *Arabidopsis thaliana* is an F-box protein required for normal patterning and growth in the floral meristem. *Plant J.* 20, 433–445.
- Shannon, S., Meeks-Wagner, D.R., 1993. Genetic interactions that regulate inflorescence development in *Arabidopsis*. *Plant Cell* 5, 639–655.
- Smyth, D.R., Bowman, J.L., Meyerowitz, E.M., 1990. Early flower development in *Arabidopsis*. *Plant Cell* 2, 755–767.
- Sundström, J.F., Nakayama, N., Glimelius, K., Irish, V.F., 2006. Direct regulation of the floral homeotic APETALA1 gene by APETALA3 and PISTILLATA in *Arabidopsis*. *Plant J.* 46, 593–600.
- von Dassow, G., Meir, E., Munro, E.M., Odell, G.M., 2000. The segment polarity network is a robust developmental module. *Nature* 406, 188–192.